JOURNAL OF MATERIALS SCIENCE **38** (2003) 269–273

Microstructure and properties of composite (B + C) diffusion layers on low-carbon steel

A. PERTEK, M. KULKA
Institute of Materials Science and Engineering, Poznan University of Technology, Pl. M.Sklodowskiej-Curie 5, 60-965 Poznan, Poland
E-mail: pertek@sol.put.poznan.pl

Combined surface hardening with boron and carbon was used for low-carbon 5120 steel. The microstructure, carbon profiles and chosen properties of borided layers produced on the carburized 5120 steel have been examined. These composite (B + C) layers are termed borocarburized layers. The microhardness profiles and wear resistance of these layers have been studied. In the microstructure of the borocarburized layer two zones have been observed: iron borides ($FeB + Fe_2B$) and a carburized layer. It has been found the depth (100–125 μm) and microhardness (1500–1900 HV) of iron borides zone. The carbon content (0.83–1.46 wt pct) and microhardness (950 HV) beneath iron borides zone have been determined. The microhardness gradient in borocarburized layer has been reduced in comparison with the only borided layer. An increase of distance from the surface is accompanied by a decrease of carbon content and microhardness in the carburized zone. The carbon and microhardness profiles of borided, carburized and borocarburized layers have been presented. A positive influence of composite layers (B + C) on the wear resistance was determined. The wear resistance of the borocarburized layer was determined to be greater in comparison with that for only borided or only carburized layers.

1. Introduction

Diffusion boriding is a thermochemical treatment that permits boride layers of good performance properties to be produced on steels [1–5]. The borided steel surfaces exhibit extreme hardness, high wear resistance and strong corrosion resistance. A prospective line for future development of this technique is the production of multicomponent and composite borided layers. These layers can be formed using fixed methods. During B-C-nitriding process [6] boron, carbon and nitrogen atoms were diffused into the surface of 1045 steel. This reduces the hardness gradient of the boride layer to the substrate and improves the mechanical and anticorrosion properties in comparison with only borided layer. In the other process [3, 7, 8] borided layers were produced using, prior to boriding, electroless (autocatalytic) nickel plating of the steel parts to be borided. The layers thus obtained show a good resistance to frictional wear and corrosion. The effect of precarburizing treatment on the morphology of the boride layer has been studied [9]. In this paper the microstructure, carbon profiles and chosen properties of borided layers produced on the previously carburized 5120 steel have been investigated. These composite diffusion layers were termed borocarburized layers.

2. Experimental procedure

Chemical composition of AISI 5120 steel used by experiments is presented in Table I.

TABLE I Chemical composition of 5120 steel

C	Mn	Si	Cr	Ni	Cu	P	S
0.22	0.70	0.28	0.80	0.13	0.11	0.015	0.022

The carburized layers have been formed in controlled carburizing atmosphere [10] at 930°C. The arrangements are shown and described in Fig. 1. The atmosphere of a fixed composition (cracked methanol with propane-butane gas) has been used. The specimens were put into the quartz tube (24) and carburized at two fixed carbon potentials (1.2 and 1.25%C) for 6 h. Carbon potential C_p was controlled by means of dew-point measuring system (16) and by pure Fe-C foils carburized until equilibrium with atmosphere was obtained. Carbon content in pure Fe-C alloy corresponds to carbon potential of atmosphere. After carburizing the specimens were slowly cooled in used atmosphere.

Gas boriding [11] was carried out by means of the apparatus shown in Fig. 2. The specimens were put into the quartz tube (2). Before boriding the system was checked to see by vacuummeter (7) that the air was removed by vacuum pump (5). A gas mixture of hydrogen and BCl_3 (up to 5 vol%) was fed through at a flow rate of 50 l/h after the furnace (1) had reached a temperature of 950°C. Then the furnace was turned up so that the specimens reached the required temperature. After heating for 2 h the furnace was moved down and

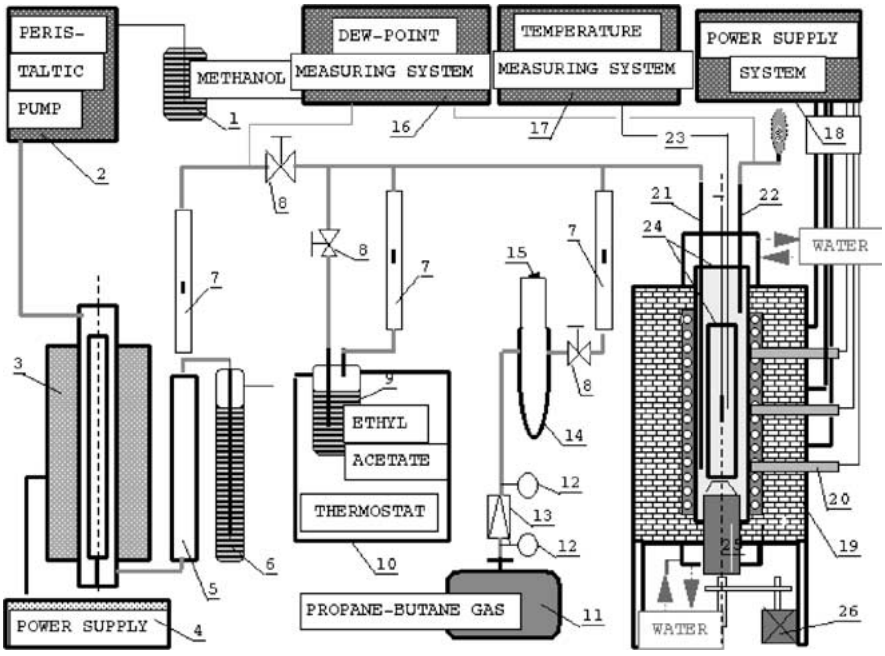

Figure 1 The arrangements used by carburizing: (1) methanol; (2) peristaltic miniflow pump; (3) generator of atmosphere; (4) power supply system; (5) water cooler; (6) manostat; (7) rotameter; (8) valve; (9) ethyl acetate; (10) thermostat; (11) bottle with propane-butane; (12) manometer; (13) pressure-reducing valve; (14) U-tube manometer; (15) ruff; (16) dew-point measuring system; (17) temperature measuring system; (18) power supply system and temperature regulation; (19) carburizing furnace; (20) regulating thermo-element; (21) gas input; (22) gas output; (23) measuring thermoelement; (24) internal and external quartz tubes; (25) ventilator; (26) motor of ventilator.

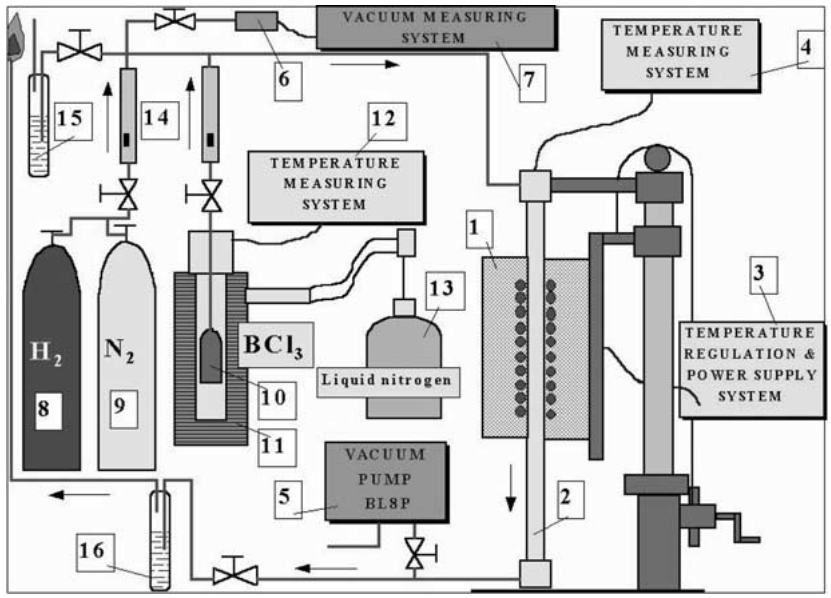

Figure 2 The arrangements used by boriding: (1) boriding furnace; (2) quartz tube; (3) power supply system and temperature regulation; (4) temperature measuring system; (5) vacuum pump; (6) vacuum measuring probe; (7) vacuummeter; (8) bottle with hydrogen; (9) bottle with nitrogen; (10) BCl_3; (11) cryostat; (12) temperature measuring system; (13) Dewar flask with liquid nitrogen; (14) rotameters; (15) manostat; (16) device for rinsing outlet gases.

the specimens were cooled in used atmosphere. The parameters of the all the thermochemical processes were selected as in Table II.

Two types of specimens were investigated. The specimens in the shape of cylinders of about 20 mm dia and 100 mm long were used in the chemical composition analysis of diffusion layers. Carbon profiles through carburized and borocarburized layers were determined by chemical analysis of successive layers. The polished cross-sections were observed by use of a SEM Philips XL 30. Carbon contents underneath the iron borides

TABLE II The parameters of thermochemical processes

	Carburizing parameters			Boriding parameters	
Type of process	C_p (wt pct)	Temp. (°C)	Time (h)	Temp. (°C)	Time (h)
Carburizing (1)	1.25	930	6	–	–
Carburizing (2)	1.20	930	6	–	–
Boriding	–	–	–	950	2
Borocarburizing (1)	1.25	930	6	950	2
Borocarburizing (2)	1.20	930	6	950	2

C_p - Carbon potential [wt pct].

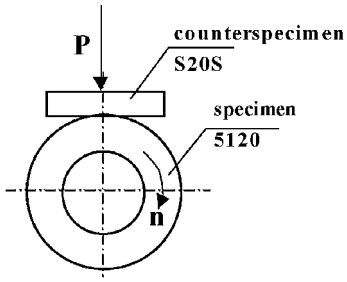

Figure 3 Scheme of wear. $P = 147$ N, rotational speed $n = 250$ min^{-1}.

after boriding and borocarburizing were measured by an EDAX X-ray microanalyser equipped with EDS, using a 35° take-off angle. The accelerating voltage was 12 kV. The detector Si(Li) with ultra thin window, standardless quantitative analysis, matrix correction algorithms ZAF for SEM bulk analysis have been applied. The second type of specimens was used to research the functional properties. To examine frictional wear resistance of the diffusion layers a research apparatus, in which a roller constitutes a sample and sintered carbide plate a countersample, has been applied (Fig. 3). The frictional tests have been made under the loading $P = 147$ N and the sample speed of 0.26 m/s, under conditions of dry friction (unlubricated sliding contact). Wear resistance has been defined as specimen mass loss per friction surface and unit of time. The coefficient of wear intensity I_z was determined as: $I_z = \Delta m/(Ft)$, where: Δm is the mass loss (mg); F is the friction surface (cm^2); t is the friction time (h). To determine microhardness profiles (Vickers method) the apparatus ZWICK 3212 B has been applied.

Before the microhardness and wear resistance tests carburized, borided and borocarburized specimens were oil quenched from 850°C and tempered at 150°C.

3. Results and discussion

3.1. Microstructure of borocarburized layers

Microstructures of cross-sections of borocarburized and hardened layers are shown in Figs 4 and 5. Two zones in borocarburized layer are visible: an iron borides zone ($FeB + Fe_2B$) and a carburized zone. The iron borides zone after borocarburizing (1) exhibits lower case depth than that obtained after borocarburizing (2). The iron borides zone ($FeB + Fe_2B$) after first process reached a thickness about 100 μm, and after second—about 125 μm. It is an effect of fixed carbon content at the surface before boriding and it is in agreement with other results [9]. The higher cementite content beneath the iron borides were observed after borocarburizing (1).

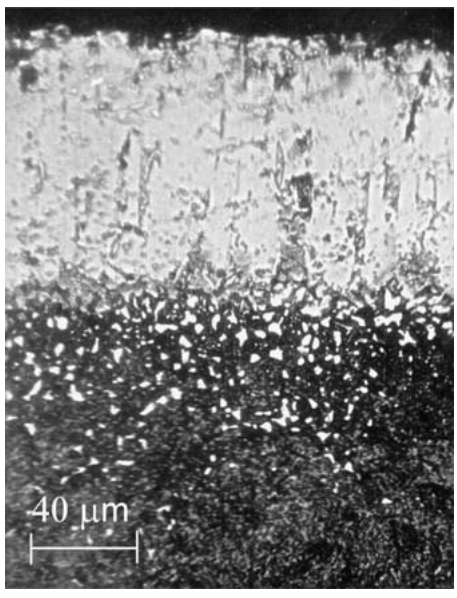

Figure 4 Microstructure of borocarburized (1) and hardened 5120 steel.

TABLE III The results of carbon content measurements

Type of process	C_s after carburizing (wt pct)	C_b after boriding (wt pct)
Carburizing (1)	2.4	–
Carburizing (2)	1.4	–
Boriding	0.22[a]	0.6
Borocarburizing (1)	2.4	1.46
Borocarburizing (2)	1.4	0.83

C_s - Carbon content at the surface after carburizing.
[a] - Carbon content in 5120 steel before boriding.
C_b - Carbon content under the iron borides after boriding.

Figure 5 Microstructure of borocarburized (2) and hardened 5120 steel.

The research results of carbon content at the surface after carburizing (C_s) and beneath iron borides after boriding (C_b) are presented in Table III.

The essential influence of chromium in 5120 steel on the carbon activity in austenite during carburizing [10] was demonstrated. The carbon content at the surface obtained after carburizing is higher, than that determined from gas composition of the carburizing atmosphere (carbon potential). The carburizing (1) at higher carbon potential (1.25%C) is accompanied by higher carbon content at the surface (2.4%C_s). After boriding of previously carburized 5120 steel (borocarburizing 1) carbon content 1.46%C_b was determined beneath iron borides. In the second case (borocarburizing 2) the carbon content 1.4%C_s and 0.83%C_b were obtained respectively.

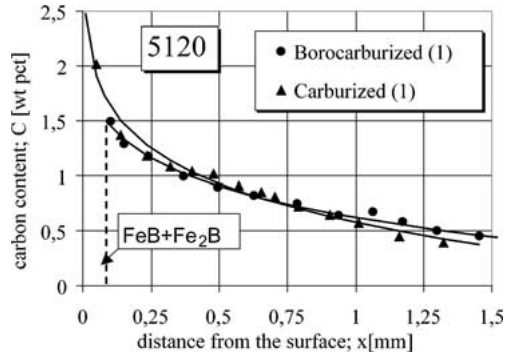

Figure 6 Carbon profiles in carburized (1) and borocarburized (1) layers.

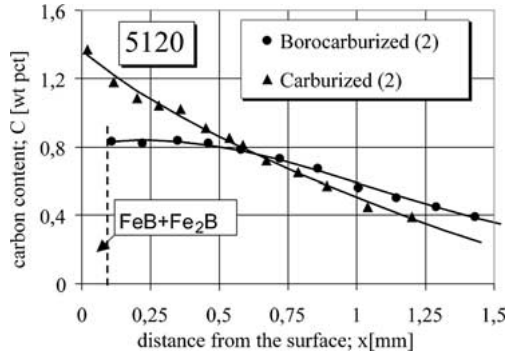

Figure 7 Carbon profiles in carburized (2) and borocarburized (2) layers.

3.2. Carbon profiles after carburizing and borocarburizing

The carbon profiles after carburizing and beneath the iron borides zone in borocarburized layers are shown in Figs 6 and 7. The carbon potential of carburizing atmosphere has an influence on carbon profiles. At higher carbon potential (1.25%) the higher carbon content at the surface and the higher case depth were obtained. During the boriding of carburized layer the carbon is moved in a core direction by following the boron diffusion front. This is also caused by the difference in carbon activity between surface area and core of steel. In effect the decrease of carbon content under iron borides and increase in the core of steel have been observed. The lower carbon content gradient underneath the iron boride zone after borocarburizing (2), than after borocarburizing (1) has been determined.

3.3. Microhardness of borided, carburized and borocarburized layers

The microhardness profiles in hardened diffusion layers up to 0.5 mm of case depth are presented in Figs 8 and 9. The highest microhardness at the surface after boriding and borocarburizing was obtained. The microhardness of the iron borides zone (FeB + Fe_2B) 1500–1850 HV has been determined. The higher microhardness (about 1850 HV) is caused by the presence of iron borides FeB in the surface zone. The lower values (about 1500 HV) are accompanied by iron borides Fe_2B. After borocarburizing (2) a slightly higher microhardness of iron borides has been observed than that after borocarburizing (1). The microhardness of hardened carburizing layer at the surface (950 HV) has been determined.

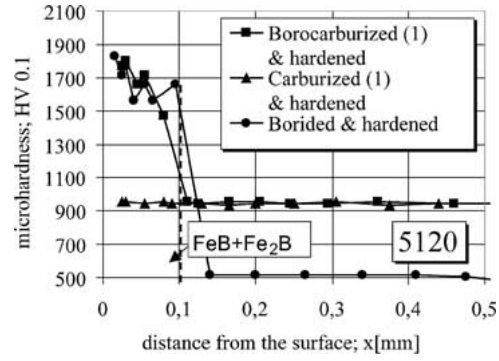

Figure 8 Microhardness profiles in hardened diffusion layers after boriding, carburizing (1) and borocarburizing (1).

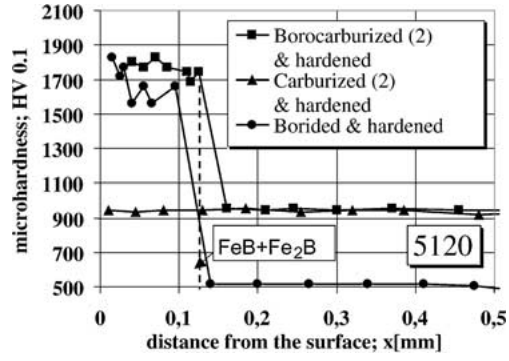

Figure 9 Microhardness profiles in hardened diffusion layers after boriding, carburizing (2) and borocarburizing (2).

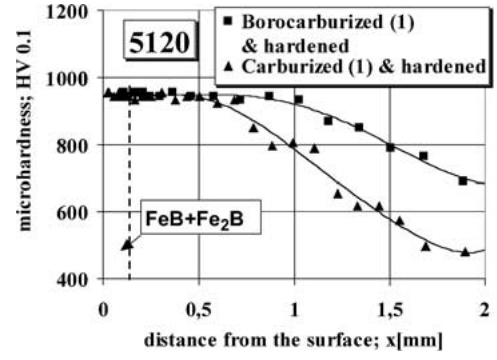

Figure 10 Microhardness profiles in carburized layer after carburizing (1) and borocarburizing (1).

A lower gradient of microhardness of the iron boride zone to the substrate in borocarburized layers in comparison with the only borided layer has been observed. The microhardness of the borocarburized layers below iron borides (950 HV) is higher than that obtained by boriding process (500 HV).

The comparison of microhardness profiles of the carburized zone after carburizing and borocarburizing (beneath the iron borides zone) are shown in Figs 10 and 11. The microhardness below the iron borides zone is the same as that obtained at the surface of only carburized layers (950 HV). An increase of the distance from the surface is accompanied by a decrease in the microhardness, but higher values were observed in case of borocarburized layers. It is related to the appearance of higher carbon contents in comparison with only carburized layers.

TABLE IV The results of wear resistance research

Type of process	Wear intensity coefficient I_z (mg/(cm^2 h))
Carburizing (1)	1.56
Carburizing (2)	1.73
Boriding	1.67
Borocarburizing (1)	1.01
Borocarburizing (2)	1.34

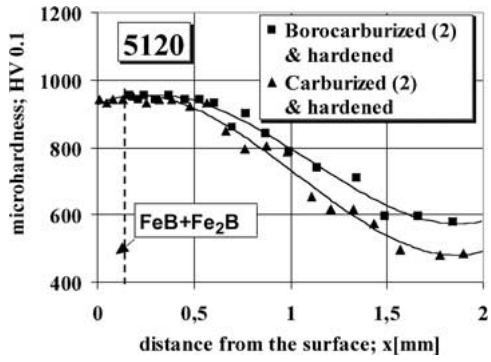

Figure 11 Microhardness profiles in carburized layer after carburizing (2) and borocarburizing (2).

3.4. Resistance to wear

The results of wear resistance research are presented in Table IV. The lowest values of wear intensity coefficient have been observed in the case of borocarburized layers. Composite diffusion layers (B + C) have a positive influence on the wear resistance. When comparing the resistance to frictional wear of the borided layers on steel previously subjected or not subjected to carburization, we can see that the borided layers formed on carburized steel show a higher resistance to frictional wear.

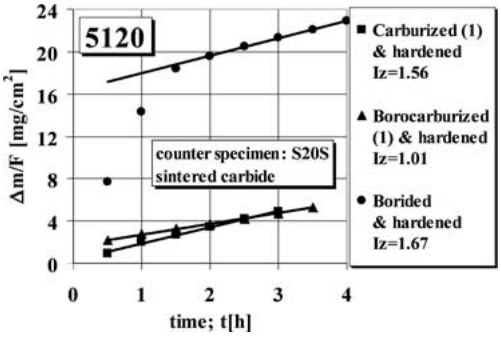

Figure 12 Weight wear of the borided, carburized (1) and borocarburized (1) layers.

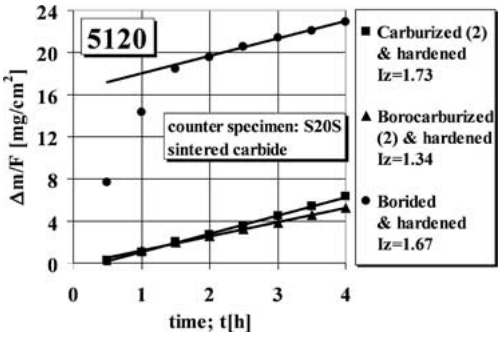

Figure 13 Weight wear of the borided, carburized (2) and borocarburized (2) layers.

The higher wear resistance of borocarburized layer has been shown in comparison to only carburized layers, too. The results of specimen mass loss on a friction surface unit in a function of friction time are shown in Figs 12 and 13. The wear intensity coefficients are defined as the directional coefficients of linear wear equations.

4. Conclusions

Combined surface hardening with boron and carbon was proposed for low-carbon 5120 steel. Gas boriding applied to parts that have been previously carburized enables the production of composite borocarburized layers. In the microstructure of borocarburized layer two zones have been observed: iron borides ($FeB + Fe_2B$) and carburized zone. The depth (100–125 μm) and microhardness (1500–1900 HV) of iron borides zone have been found. The depth of this zone and carbon profile underneath can be controlled by carburizing parameters before boriding. Higher thickness of iron borides zone and lower gradient of carbon in carburized zone were observed after borocarburizing (2). In this case the slightly higher microhardness of the iron borides zone and the lower carbon content underneath have been observed, too. The gradient of microhardness of the iron borides zone to the substrate in borocarburized layers has been reduced in comparison with that of an only borided layer. The carbon contents (0.83–1.46 wt pct) and microhardness (950 HV) below iron borides zone have been determined. An increase of distance from the surface is accompanied by a gradual decrease of carbon content and microhardness in carburized zone. An advantageous influence of composite (B + C) layers on the frictional wear resistance has been found. The essentially higher wear resistance of borocarburized layer has been obtained in comparison with only borided or only carburized layers.

References

1. A. GRAF VON MATUSCHKA, "Borieren" (Carl Hanser Verlag, Munchen, Wien, 1977).
2. B. VENKATARAMAN and G. SUNDARARAJAN, *Surf. Coat. Technol.* **73** (1995) 177.
3. T. WIERZCHOŃ and P. BIELIŃSKI, *Mater. Manuf. Process.* **10** (1995) 121.
4. H. J. HUNGER and G. TRUTE, *Heat Treatment of Metals* **21**(2) (1994) 31.
5. C. H. XU, J. K. XI and W. GAO, *J. Mater. Process. Technol.* **65** (1997) 94.
6. P. X. YAN and Y. C. SU, *Materials Chemistry and Physics* **39** (1995) 304.
7. T. WIERZCHOŃ, P. BIELIŃSKI and K. SIKORSKI, *Surf. Coat. Technol.* **73** (1995) 121.
8. K. SIKORSKI, T. WIERZCHOŃ and P. BIELIŃSKI, *J. Mater. Sci.* **33** (1998) 811.
9. M. R. TOROGHINEZHAD, M. SALEHI and F. ASHRAFIZA-DEH, *Mater. Manuf. Process.* **12**(1) (1997) 117.
10. M. KULKA, M. PRZYŁECKA and W. GESTWA, *Materials Science Forum. Trans Tech Publications, Switzerland*, **163–165** (1994) 87.
11. A. PERTEK, *Materials Science Forum. Trans Tech Publications, Switzerland* **163–165** (1994) 323.

Received 9 January
and accepted 24 September 2002